Mathematical Model and Experimental Characterization of Vertically Stacked Capacitive Tactile Sensors

Giulia Baldini, Marco Staiano, Francesco Grella, Mattia Frascio, Perla Maiolino, *Member, IEEE*, and Giorgio Cannata, *Member, IEEE*

Abstract—**Capacitive sensors are widely used in robotics for their compactness, high resolution, high sensitivity, and large dynamic range. In this article, we present a design solution for the manufacturing of capacitive tactile sensors with enhanced dynamic range and sensitivity. Herein, we adopted the approach of exploiting the vertical direction of the sensors by creating stacks of capacitors. The validation of the proposed model is conducted by means of finite element simulations and the effectiveness of stacked capacitors in suboptimal configurations has been experimentally tested by using inkjet printing and spin coating-based fabrication techniques. Results show that these sensors exhibit an enhanced dynamic range and sensitivity with respect to common single capacitors, for a given sensors area budget. Sensitivity increases of 235% passing from one-stack to two-stack capacitors (from 5.75 to 19.3 fF/kPa) and a growth of 23% from two-stack to three-stack capacitors (from 19.3 to 23.7 fF/kPa). These results suggest that the proposed methodology could be adopted for designing tactile sensors with higher spatial resolution and higher transduction sensitivity and dynamic range, in the perspective of an integration over large areas.**

Index Terms—**Capacitive tactile sensing, dynamic range, inkjet printing, robotics, sensitivity, stack.**
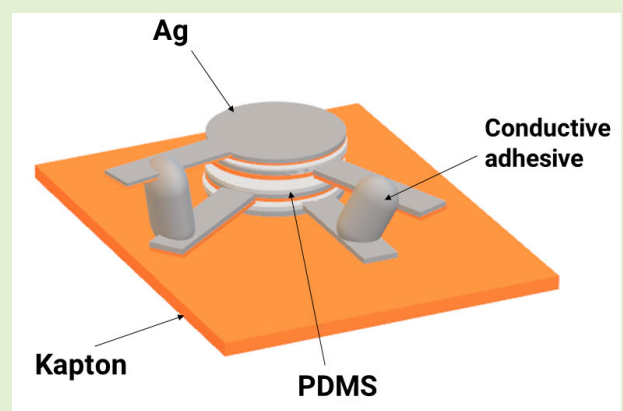
I. INTRODUCTION

ROBOTS have gathered a lot of attention in the last two decades, and they have been playing a bigger part in the industrial scene and in everyday life. Using the human as a model, advanced technology and great progresses in mimicking sensory capabilities have been demonstrated [1],

Giulia Baldini, Marco Staiano, Francesco Grella, and Giorgio Cannata are with the Mechatronics and Automatic Control Laboratory, University of Genoa, 16145 Genoa, Italy (e-mail: giulia.baldini@edu.unige.it; marco.staiano@edu.unige.it; francesco.grella@edu.unige.it; giorgio.cannata@unige.it).

Mattia Frascio is with the Department of Mechanical Engineering (DIME), University of Genoa, 16145 Genoa, Italy (e-mail: mattia.frascio@unige.it).

Perla Maiolino is with the Oxford Robotics Institute, OX2 6NN Oxford, U.K. (e-mail: perla.maiolino@eng.ox.ac.uk).

[2]. Tactile information, such as the magnitude and direction of a contact force, temperature, humidity, and texture, can be obtained by robots equipped with tactile sensors, which is crucial for secure grasps, path planning, and obstacle avoidance in unstructured environments [3], [4]. In addition, reliable touch sensors are required for both object manipulation activities and safe human–machine interaction [5]. Capacitive sensing is one of the most common principles used in robotic tactile sensing. The capacitance of a parallel plate capacitor is expressed as $C = (\epsilon_0 \epsilon_r A/d)$, where A is the overlapping area of the two electrodes, ϵ_0 is the permittivity of vacuum, ϵ_r is the relative permittivity of the dielectric layer, and d is the distance between the electrodes (thickness). Researchers are interested in capacitive sensors because of their great sensitivity, resolution, costs, and read-out electronics.

For a good response, capacitive sensors require a wide dynamic range, defined as the ratio between the maximum and the minimum value that the sensor can detect. The dynamic range can be increased by maximizing the sensor capacitance (C) and it is strictly correlated to the sensitivity (S) of the transducer, expressed as the ratio between the variation in

capacitance for a given variation of contact pressure. The capacitance C can be increased by decreasing the sensor thickness and/or by increasing the sensor area. Unfortunately, both approaches bring to some drawbacks. In particular, the decrease in the sensor thickness is limited by the technology used to manufacture the sensor. Furthermore, the increase in the sensor area can lead to space problems on small surfaces. There are works in literature that proposed methods to enhance the dynamic range of capacitive tactile sensors [6], [7], [8], [9], [10]. An interesting approach is the exploitation of the vertical direction. Results from the works of [11], [12], [13], [15], and [14] show that this design for capacitive sensors reduces the projective area taken on the xy plane for enhanced spatial resolution and sensitivity and it can be used for extreme miniaturizations. Jen et al. [16] developed and characterized a capacitive tactile sensor that simultaneously supports high detection sensitivity and high spatial resolution with a hollow dielectric structure, by vertically stacking two capacitors. Liu et al. [17] and Yin et al. [18] made significant advances in flexible capacitive pressure/tactile sensors such as low-voltage organic transistors for sensitive pressure sensing and wearable applications by combining the advantages of different dielectrics.

Building on the mentioned approaches, this work aims to maximize the dynamic range of capacitive tactile sensors and their sensitivity by exploiting the vertical direction and creating stacks of more than two capacitors. If the previously mentioned works propose a specific solution, the goal of this article is to develop a model that allows to choose the design parameters and to evaluate different stacking options to reach the desired sensitivity. This work provides the following contributions.

1) The development of a mathematical model for tactile capacitive sensors, in order to find a configuration to increase their sensitivity with respect to the common single capacitors.
2) The validation of the mathematical model with finite element simulations, by studying the sensor's responses.
3) A straightforward method for manufacturing and characterizing vertically stacked capacitive tactile sensors.
4) Static and dynamic experimental analyses to validate the sensitivity and dynamic range increase on inkjet-printed sensors.

The remainder of the article is organized as follows.

Section II presents the theoretical modeling of capacitive sensors. The aim is to demonstrate that the sensitivity of a single capacitance is lower with respect to a stack of capacitors. The model allows to give guidelines for the design of new layouts in order to increase the performance of this class of sensors. Section III presents the results of finite element analysis for validating the proposed mathematical model and for studying the mechanical behavior of the dielectric material, also introducing nonlinear simulations to compare the results with the experiments. In Section IV, we describe the manufacturing process adopted to build the stacked capacitors. Section V presents the static and dynamic characterization of
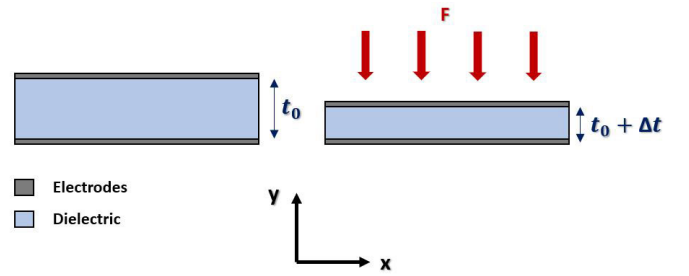

Fig. 1. Schematic of the working principle of a capacitive tactile sensor. An external force applied on the plate at time t_0 induces a deformation of the dielectric which results in a measured capacitance variation.

the sensor with the respective results. Conclusion is described in Section VI.

II. MATHEMATICAL MODEL OF A CAPACITIVE TACTILE SENSOR

As anticipated in Section I, in order to increase the dynamic range and the sensitivity of the response, we propose the development of stacked parallel capacitance. The sensitivity of capacitance measurements is dependent on the thick values of the capacitance. For a given thickness, the first goal is to evaluate how thick the layers composing the stack must be to optimize sensor response, respecting design and manufacturing constraints. The second purpose of the demonstration is to indicate how many capacitors have to be stacked in order to maximize the resulting sensitivity.

A. Capacitive Sensors Principle

As shown in Fig. 1, the variation of the pressure applied on the sensor due to the force F uniformly distributed on the transducer area A can be written as follows:

$$\Delta P = -\frac{F}{A} \tag{1}$$

where the pressure variation $\Delta P = P - P_0$ is supposed to be uniform on the whole sensor area. P is the applied pressure and P_0 is any possible equilibrium pressure (e.g., preloading pressure or atmospheric pressure in the case of pressure-compensated sensors). We start to share how an applied pressure is uniformly distributed on the sensor surface, and we can compare the deformation of the dielectric material of the capacitive sensor with the deformation of the *equivalent spring*, using the following formula:

$$F = k \cdot \Delta t, \quad \Delta t < 0 \tag{2}$$

where k is the elastic constant of the *equivalent spring*, representing the linearized effect of the applied force in terms of the sensor deformation. $\Delta t = t - t_0$ is the displacement, t is the resulting thickness of the dielectric due to the pressure applied on the transducer, and t_0 is the initial thickness.

Using the standard stiffness engineering model [19], [20], we have that

$$k = \frac{E \cdot A}{t_0} \tag{3}$$

where E is the Young's Modulus of the material.

By substituting the value of F computed from (1) in to (2) and using the definition of k of (3) we obtain the following equality:

$$-A \cdot \Delta P = \frac{E \cdot A}{t_0} \cdot \Delta t. \tag{4}$$

Which can also be rewritten as follows:

$$\frac{\Delta t}{t_0} = -\frac{\Delta P}{E} \tag{5}$$

assuming a linear stress-strain relationship for the material used to build the sensor. Let us now consider the nominal value of the sensor capacitance in the absence of contact pressure. The value is C_0 and it is expressed as follows:

$$C_0 = \gamma \frac{A}{t_0}. \tag{6}$$

$\gamma = \epsilon \epsilon_r$, where ϵ and ϵ_r are the vacuum electric permeability and the dielectric constant of the material used, respectively. Once pressure is applied to the sensor, the resulting capacitance becomes

$$C = \gamma \frac{A}{t_0 + \Delta t} \tag{7}$$

under the assumption that the transducer area does not change under the effect of contact pressure. The difference between C and C_0 can then be written as follows:

$$\begin{aligned}
\Delta C = C - C_0 &= \gamma \frac{A}{t_0 + \Delta t} - \gamma \frac{A}{t_0} \\
&= \gamma A \left(\frac{1}{t_0 + \Delta t} - \frac{1}{t_0} \right) = \gamma A \left[\frac{-\Delta t}{t_0 (t_0 + \Delta t)} \right] \\
&= \frac{\gamma A}{t_0} \left[\frac{-\Delta t}{t_0 + \Delta t} \right] = -C_0 \left[\frac{\Delta t}{t_0 + \Delta t} \right].
\end{aligned} \tag{8}$$

By using (5), we can write (8) as follows:

$$\Delta C = C_0 \frac{t_0 \frac{\Delta P}{E}}{t_0 - t_0 \frac{\Delta P}{E}} = C_0 \frac{t_0 \Delta P}{t_0 E - t_0 \Delta P} = C_0 \frac{\Delta P}{E - \Delta P}. \tag{9}$$

B. Two-Layered Stacked Capacitance

In Section II-B, we analyze the dielectric thickness requirement by considering a capacitive sensor configured as parallel capacitance (stack), composed of two layers of dielectric material, as in Fig. 2.

For capacitive sensors, in general, the dielectric greatly affects the response of the device [21]. In this article, we only considered the effect of the dielectric in terms of its deformation. From (9), can define the total variation of the stack as the sum of the variation of the two capacitors

$$\begin{aligned}
\Delta C &= C_{1_0} \frac{\Delta P}{E - \Delta P} + C_{2_0} \frac{\Delta P}{E - \Delta P} \\
&= (C_{1_0} + C_{2_0}) \frac{\Delta P}{E - \Delta P} = C_0 \frac{\Delta P}{E - \Delta P}
\end{aligned} \tag{10}$$

where $C_0 = C_{1_0} + C_{2_0}$ is now the total capacitance of the stack at rest. Suppose we want to design a stacked sensor with these characteristics such that the total thickness of the sensor (design parameter) is defined as equal to t_{tot}. In this
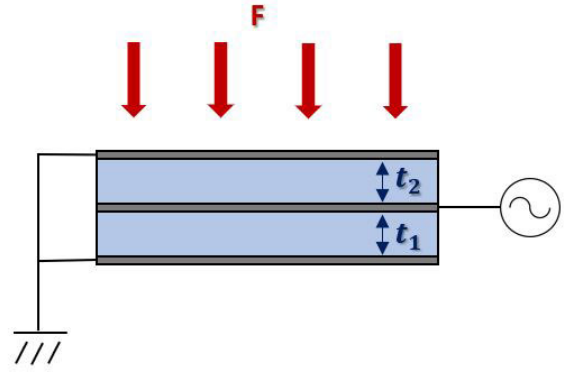

Fig. 2. Schematic of a capacitive sensor configured as parallel capacitance. The thickness variation of the electrodes is always negligible compared to the dielectric deformation.

case, the thicknesses of the two capacitors t_1 and t_2 become the design parameters. With these considerations, we can write C_0 as follows:

$$C_0 = \gamma A \left[\frac{1}{t_1} + \frac{1}{t_2} \right] = \gamma A \frac{t_1 + t_2}{t_1 t_2} = \gamma A \frac{t_{\text{tot}}}{t_1 (t_{\text{tot}} - t_1)}. \tag{11}$$

So, for a given capacitor thickness, the goal is to decide how much t_1 and t_2 should be

$$\frac{t_1}{t_{\text{tot}}} + \frac{t_2}{t_{\text{tot}}} = 1. \tag{12}$$

By defining

$$\frac{t_1}{t_{\text{tot}}} = x, \qquad \frac{t_2}{t_{\text{tot}}} = 1 - x \tag{13}$$

we can write (11) using (12) and (13)

$$C_0 = \gamma A \frac{1}{x(1-x)}. \tag{14}$$

The sensitivity S is defined as the ratio between the variation of capacitance ΔC and the variation of the exerted pressure ΔP (i.e., the stress)

$$S = \frac{\Delta C}{\Delta P}. \tag{15}$$

The sensitivity is proportional to ΔC and by (10) to C_0. Therefore, for a given ΔP, C_0 must be maximized.

Fig. 3 shows the trend of C_0 with respect to the layer thickness, expressed with the variable x (minimum possible thickness for the dielectric).

The formulation of the computation of the maximum of C_0 must be constrained since the minimum value of x is indeed a physical constraint that might depend on the technology used for the manufacturing of the sensor and on the characteristics of the material involved in the design.

From this result, we can say that the decreasing of the layer thicknesses improves the output and so the sensitivity of the capacitive sensor.
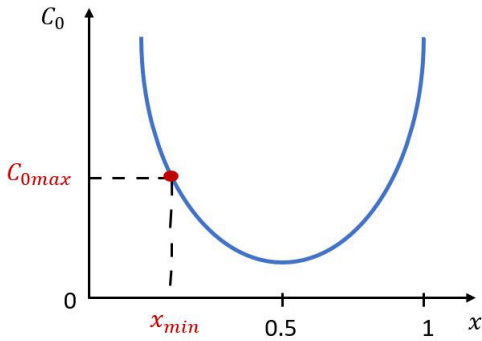
Fig. 3. Plot showing the initial capacitance C_0 with respect to the layer thickness. The red dot represents qualitatively the tradeoff between achieved capacitance with respect to the minimum achievable layer thickness.

TABLE I
MOST RELEVANT DIELECTRIC MATERIAL PROPERTIES

Young's Modulus (E)	200 [kPa]
Poisson Ratio (ν)	0.49
Dielectric Permittivity (ϵ_r)	2.75
Shear modulus for neo-Hookean model (μ)	42 [kPa]

C. Three-Layered to N-Layered Stacked Capacitance

In order to generalize to the case of an N-layer stack (N-stack), let us consider as an example the case of a three-stack. Using the same notation of Section II-B, we define as x_1, x_2, and x_3 the normalized thicknesses of the three layers t_1, t_2, and t_3 with respect to the total expected sensor thickness t_{tot}. Then the following optimized problem must be solved:

$$\max \ C_1 + C_2 + C_3$$
$$\text{s.t. } x_1 + x_2 + x_3 = 1$$
$$x_i > x_{\min} \quad \forall i. \tag{16}$$

In order to find a maximum of the above cost function, consider a feasible choice for x_1, x_2, and x_3 and assume (without loss of generality) x_1 fixed. Then following the rationale used in Section II-B, it is straightforward to verify that

$$x_2 = \min$$
$$x_3 = (1 - x_1) - x_{\min} \tag{17}$$

maximizes $C_2 + C_3$. Since C_2 cannot be increased further, x_2 can be fixed and the above rationale can be repeated for x_1 and x_3 so that it can be

$$\begin{cases} x_2 = x_{\min} \\ x_1 = x_{\min} \\ x_3 = 1 - 2x_{\min}. \end{cases} \tag{18}$$

This result eventually leads to a feasible solution to maximize the capacitance of the three-stack. It is also quite easy to check that for a given transducer thickness t_{tot}, the capacitance of a three-stack is higher than a two-stack one. The dimension above suggests that for a given thickness t_{tot}, the layers should have the following distribution:

$$\begin{cases} x_1 = x_{\min} \\ x_{N-1} = x_{\min} \\ x_N = 1 - (N - 1)x_{\min}. \end{cases} \tag{19}$$

The formal proof is in Appendix.

III. FINITE ELEMENT SIMULATIONS

In this section, we describe simulations performed with the finite element method to validate the mathematical model presented in Section II and to explain the mechanical behavior of the dielectric material, also modeling the nonlinear effect featuring the real system. On one hand, the linear simulated model is useful to validate the models discussed in Section II; on the other hand, the nonlinear simulated model is important to compare the finite element results with the experimental ones presented in Section IV. First, we define the sensors model, which is essential to simulate the sensor response. Then, we compute the sensor's finite element responses with their corresponding sensitivity and we compare the results between a single capacitor and stacks of capacitors to demonstrate that a stack performs better than a single capacitance.

A. FEM Sensor Model

Practical guidelines for the implementations of capacitive tactile sensors have been presented in [22]. The geometry and the material properties used for the simulated models have followed those guidelines and are related to existing tactile sensors implementation [36]. The simulated transducer is a single circular taxel with a diameter $d = 4$ mm. Tests in Section III-B, which are used to validate the mathematical demonstration, include models with the same thickness $t_0 = 1$ mm. Tests in Section III-C, which are used to study the mechanical behavior of the dielectric material, include models with different thicknesses, which increase every time we add a capacity in parallel to the stack. In this case, each capacitance has a thickness $t = 100$ μm. The choice of the dielectric and conductive layer materials is consistent with the materials used for the experimental tests described in Section IV. In particular, the dielectric is made of polydimethylsiloxane (PDMS), and silver ink is used for the conductive capacitor plates and electrodes. The mechanical characteristics of the conductive layers are assumed negligible and not modeled in the FEM simulations. For the nonlinear mechanical analysis, we used a neo-Hookean constitutive model for the PDMS. Table I summarizes the most relevant material properties of the dielectric material used, which are as follows.

1) The Young's modulus, defined as $E = (\sigma/\epsilon)$, where σ and ϵ are the material's stress and strain, respectively [28], is used to compute the elastomer strain under an exerted pressure.
2) The Poisson's ratio (ν) is a measure of the Poisson effect originating from the elastomer expansion along the direction normal to pressure application.
3) The dielectric permittivity (ϵ_r), which impacts on capacitance variations [22] and so on the sensor sensitivity.

B. FEM Validation of the Mathematical Model

The computational physics suite *COMSOL Multiphysics* has been used to implement the models and performance simulations, and simulation results have been further analyzed with *MATLAB*. For the simulations, two classes of contacts have been selected, following [30] and [22]. The first class is referred to as *gentle touch* and is characterized by contact pressures in the 0–10 KPa range, whereas the second class, *manipulation-like touch*, refers to pressures in the 10–100 KPa range.

Looking at the consideration of Section II, we want to validate through FEM: 1) the optimal layer distribution and 2) the maximization of the performances by increasing the number of layers. For the sake of simplicity, in all models, the sensitivity has been calculated as the angular coefficient of the linear fit curve, which can cover all the ranges, with a maximum pressure of 100 kPa, from gentle touch to manipulation-like touch.

1) Optimal Layer Distribution: Let us now consider two models, which represent a stack with the same total thickness $t_0 = 1$ mm composed of four layers. In the first case, the layers have the same thickness, in the second case, the layers are distributed according to the analysis of Section II, assuming a minimum thickness of 100 μm. Fig. 4(a) and (b) shows the two stack configurations in the case of uniform pressure applied on the top layer of 100 kPa. Fig. 4(c) shows the finite element response of the first configuration, while Fig. 4(d) shows the finite element response of the second configuration. For validation, the models have been considered linear. By comparing the two finite element results, the second case has a 7% increase in sensitivity with respect to the first case. This further validates the first part of the mathematical demonstration, on which we propose the optimal layer distribution to increase the sensor response.

2) Maximization of the Performances by Increasing the Number of Layers: Let us now consider the other two models, which represent a stack composed of four layers and a stack composed of six layers, with the same total thickness $t_0 = 1$ mm, and both with the optimized layer configuration. For the four-stack capacitor, we consider the best configuration of Section III-B.1, and so we refer to Fig. 4(b) for the model and to Fig. 4(d) for the response. Fig. 5(c) shows the six-layer stack and Fig. 5(a) shows the finite element response of the six-stack model. Also in this case, for the validation, we consider linear models. By comparing the two finite element results, the six-layer stack has a greater sensitivity with respect to the four-layer stack. This comparison tells us that by increasing the number of layers in optimal configuration by 50%, a sensitivity variation of 130% is produced.

In order to show the effectiveness of the optimal configuration, we also compared the case of four layers of equal thickness [see Fig. 4(a)] with the case of six layers of equal thickness [see Fig. 5(b)]. The results of these two nonoptimal configurations are shown in Figs. 4(c) and 5(d). In this case, a sensitivity variation of 120% is produced.

Through the tests and comparisons described in Section III-B, we have validated the entire mathematical demonstration. We can state that the manufacturing of sensors composed of stacked capacitance could lead to an improvement in the performance of capacitive sensors. Moreover, each layer has to be designed according to the optimal distribution explained above.

C. FEM Analysis on the Mechanical Behavior of the Dielectric Material

In Section III-B, the analysis aims to demonstrate that more optimized stacked capacitors have good performances. In this section, we focus on the most technologically tractable case, in which layers have all equal thicknesses. So, we work with nonoptimal configurations from the layout point of view. In this case, all the elements necessary to make the results comparable with the experimental analysis have been introduced into the FEM. In particular, in addition to the PDMS as a dielectric, kapton was also added in the simulations, as in the experiments the sensors present both materials to form the dielectric. For the models, a single capacitor, a two-stack capacitor, and a three-stack capacitor have been considered. The first simulation test refers to the analysis of the response of a one-stack and two-stack, and the second simulation test refers to the analysis of the response of a two-stack and three-stack, in order to understand how the dielectric is compliant under the action of a uniform pressure applied on the surface area. Figs. 6(a), 7(a), and 8(a) show the mechanical responses of one-stack, two-stack, and three-stack, respectively, in terms of dielectric total displacement under the maximum pressure applied. The initial values of the single capacity (C_{0_1}), of the two-stack (C_{0_2}), and of the three-stack (C_{0_3}) are 3.65, 7.29, and 10.9 pF, respectively.

Fig. 9 shows the ideal sensors' output and their corresponding sensitivity in the linear case. More detailed information are given in Figs. 6(b), 7(b), and 8(b) which show the ideal sensors output and their corresponding sensitivity in the nonlinear case. This is a more real representation of the sensor's response, and for this reason, we will consider these values as a reference to compare them with the experimental results. Results from the neo-Hookean model show that the sensitivity has an increase of the 90% passing from a single capacitor ($S = 8.9$ fF/kPa) to two-stack ($S = 16.9$ fF/kPa), and an increase of 48% passing from a two-stack to a three-stack ($S = 25$ fF/kPa). The sensitivity has an increase of 180% if we pass from a single capacitor to a three-stack capacitor. Also, in this case, the sensitivity will increase every time we add a capacity in parallel to the stack.
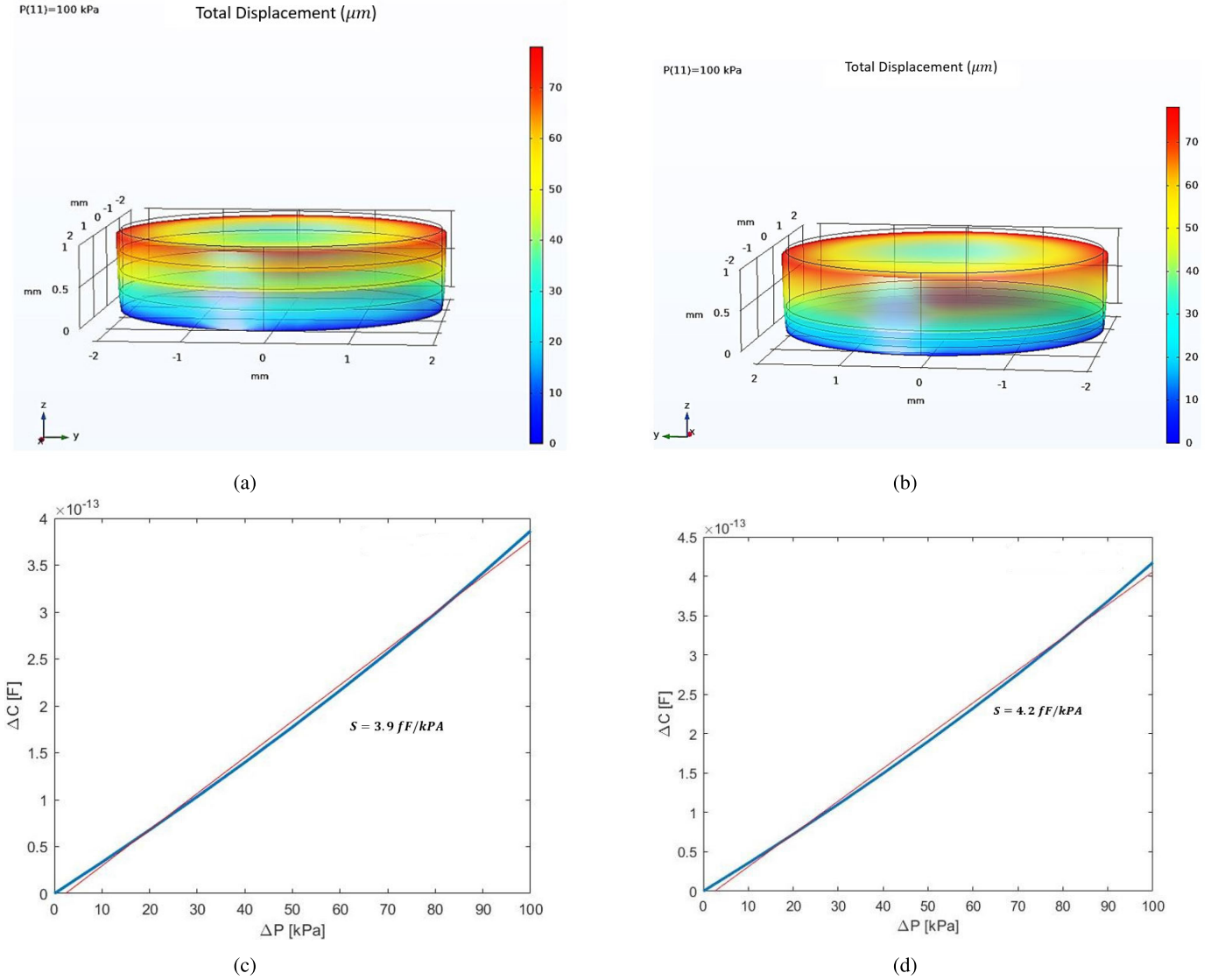
Fig. 4.   (a) Simulation for a four-stack capacitor with $t_{tot} = 1$ mm and $t_1 = t_2 = t_3 = t_4 = 250$ μm. (b).Simulation for the four-stack capacitor with $t_{tot} = 1$ mm and $t_1 = t_2 = t_3 = 100$ μm and $t_4 = 700$ μm. (c) Computed change of capacitance ΔC for a change of applied pressure ΔP for the case of (a). (d) Computed change of capancitance ΔC for a change of applied pressure ΔP for the case of (b).

IV. EXPERIMENTAL MANUFACTURING

In this section, we first show the manufacturing procedures used to make a single capacitor and stacks of capacitors (all with a diameter of 4 mm, as for the simulation models). Then, we present the characterization procedure used to compute the parameters required to validate the finite element simulations of Section III-C. The manufacturing process is based on the use of two techniques: inkjet printing and spin coating. The peculiarity of this approach is that it can be potentially used to obtain stacks of several capacitors in parallel and the procedure can be customized to optimize the sensors covering different surfaces. In this work, three kinds of sensors have been manufactured and their performances have been analyzed. The characteristics of a one-stack capacitor, the output of a two-stack capacitor, and the output of a three-stack capacitor have been computed and the results have been compared with those obtained from the simulations.

A. Single-Capacitance Tactile Sensor

1) Dielectric Preparation: Sylgard 184 (Dow Corning) is used as the dielectric material. The PDMS base and the curing agent is mixed in a 10:1 ratio (base to catalyst) in all experiments and steered for 2 min. Then, the PDMS is placed in vacuum desiccators for degassing (10–13 min). Then, a thin layer of PDMS has been deposited on the capacitor substrate by spin coating. As discussed in [31], a thickness of 25 μm guarantees excellent electrical insulation between the conductive layers. The PDMS thickness mainly depends on spin speed and duration [32], [33]. In this work, this thickness has been obtained by depositing in sequence two layers of PDM, each obtained through a spin coating with a speed of 2000 r/min and a duration of 5 min. With these parameters, each layer has a thickness of $\sim$12 μm and so the total dielectric thickness is $\sim$24 μm.

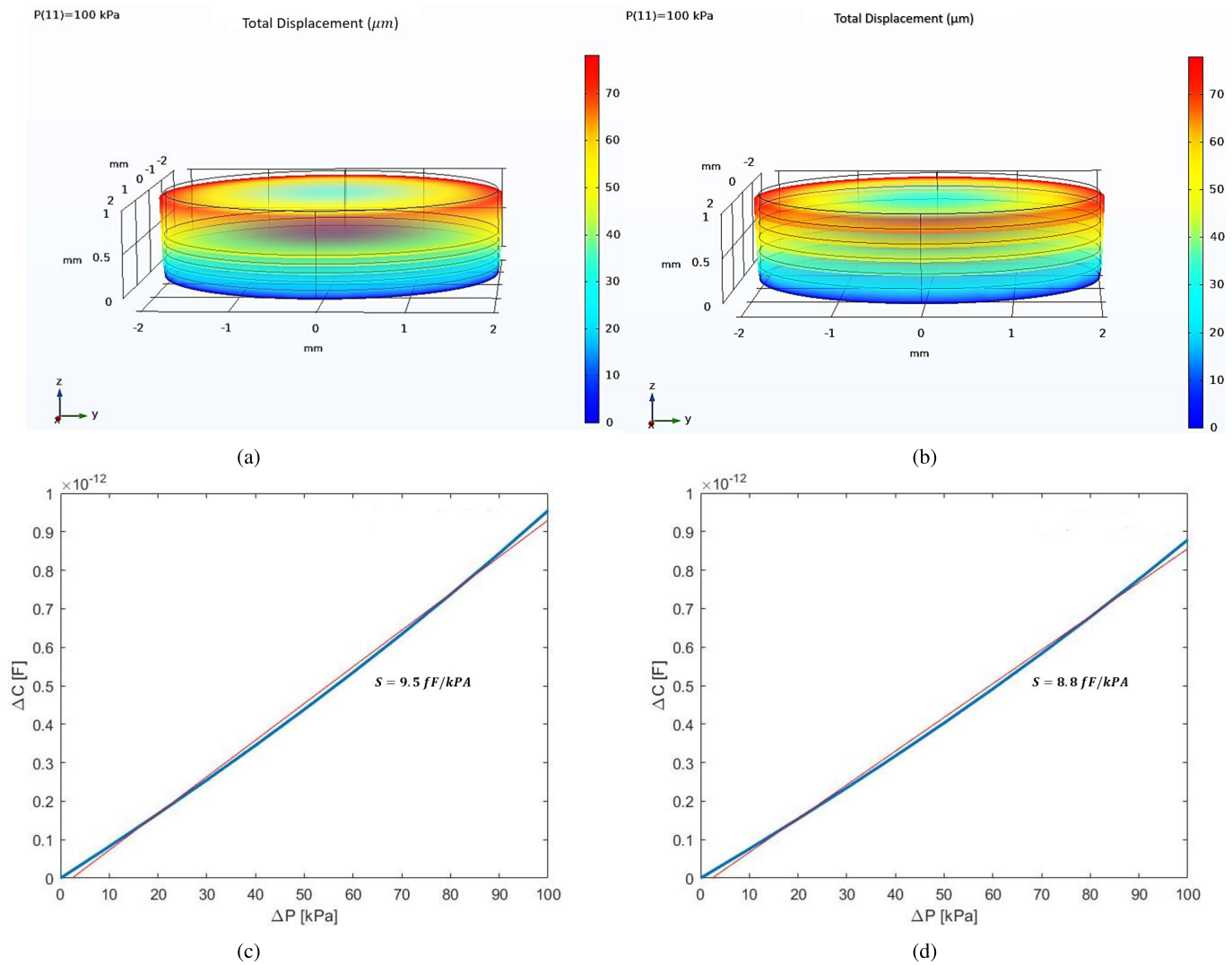The dielectric preparation is the same also in the case of the stacked capacitors described later.

Fig. 5. (a) Simulation for the six-layer stack with $t_{tot} = 1$ mm and $t_1 = t_2 = t_3 = t_4 = t_5 = 100$ μm and $t_6 = 500$ μm. (b) Simulation for the six-layer stack with $t_{tot} = 1$ mm and $t_1 = t_2 = t_3 = t_4 = t_5 = t_6 = 100$ μm. (c) Computed change of capacitance ΔC for a change of applied pressure ΔP for the case of (a). (d) Computed change of capacitance ΔC for a change of applied pressure ΔP for the case of (b).

2) Device Fabrication: The capacitor substrate consists of a suitably cleaned kapton sheet (75 μm thick). Two layers of silver nanoparticle ink (Ag NP ink, SunTronic[1] EMD5730) have been inkjet printed directly on the substrate with the commercial inkjet printer Dimatix DMP-2850 Fujifilm. The printed substrate is briefly placed on a hot plate to evaporate the solvent until the silver of the ink emerges. After that, the curing is terminated in an oven at 150 °C for 30 min. Subsequently, the PDMS is spin-coated (as discussed in the above paragraph Section IV-A1) on top of the conductive layer and oven cured at 120 °C for 25 min allowing the solvent to evaporate and cross-link the PDMS. At the same time, another identical conductive pattern is inkjet printed on a second kapton substrate and, after the curing phase, is placed on top of the dielectric material, placed on the first substrate, to form a single capacitance. In the dashed rectangle of Fig. 10

it is shown that the fabrication process and Fig. 11(a) shows the vertical section of the structure.

B. Stacked-Capacitance Tactile Sensors

1) Device Fabrication: Starting from the manufacturing of the single capacitance, stacks of N capacitors can be built by following the fabrication process which is summarized in Fig. 10. This method allows one to stack one capacitance on top of the other, forming a stack of capacitors in parallel. Each capacitor is manufactured with the aforementioned fabrication process (see Section IV-A2). In order to obtain a set of capacitors in parallel, all the odd layers must be electrically connected together as well as all the even armatures. To the same, the printed pattern of each armature is formed by a circle and an extruded electrode which will be used to interconnect the remaining layers. From the final transducer, the sensor is composed of $2N$ right electrodes and $2N - 1$ left electrodes. All the right electrodes are electrically connected with each other with a conductive resin (MG Chemicals 842UR) and
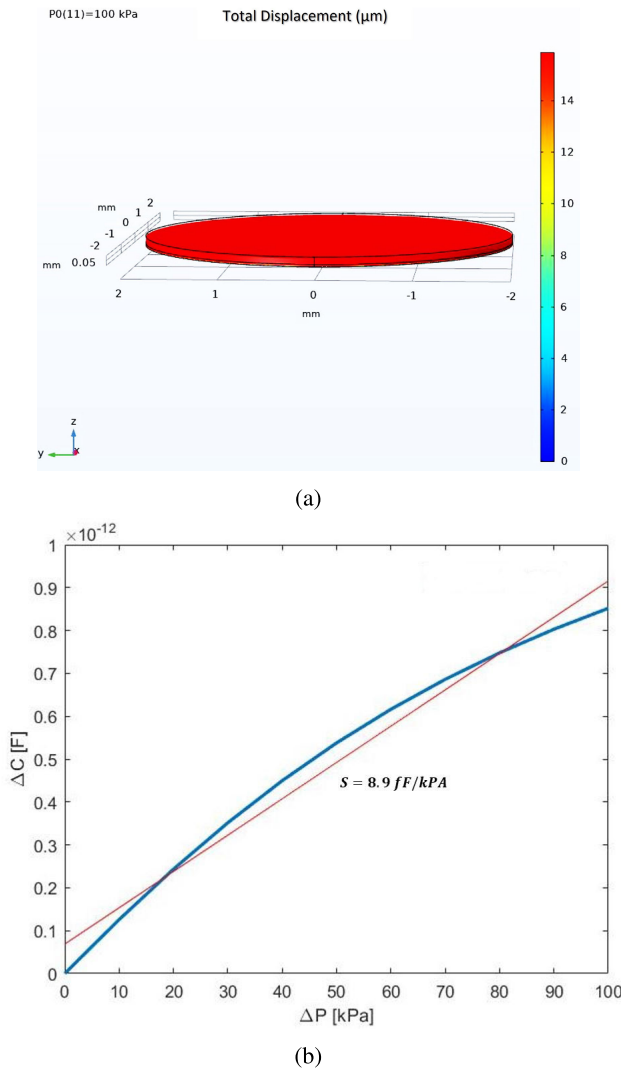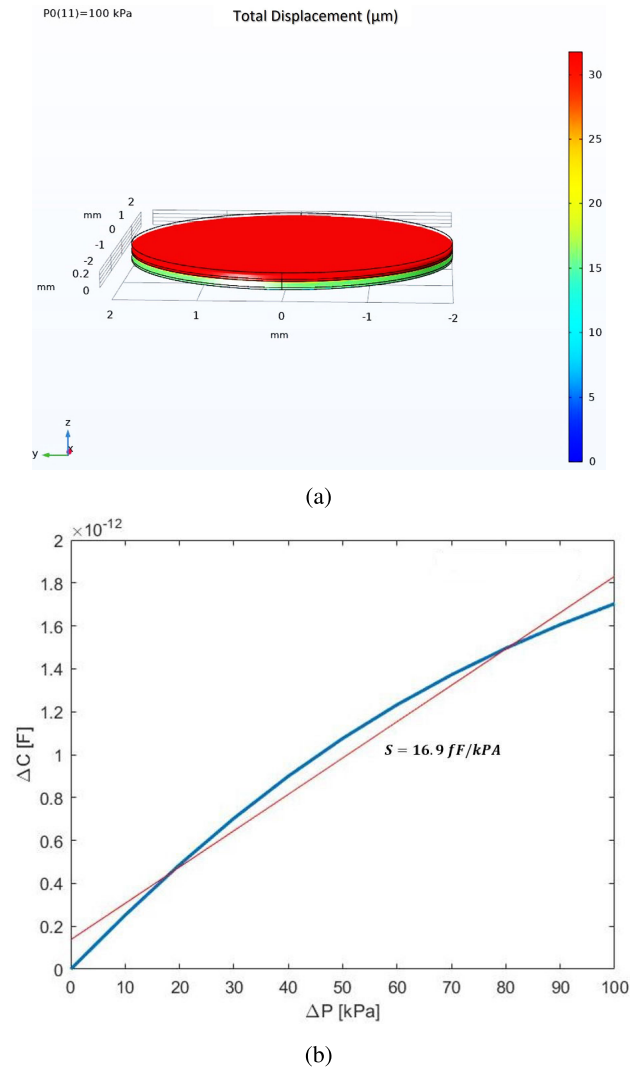
[1]Registered trademark.

(a)

(b)

Fig. 6.   (a) Behavior of the one-stack capacitor in terms of dielectric total displacement under a range of pressures applied. (b) Pressure/capacitance characterization obtained from finite element simulation with the corresponding sensitivity in the case of one-stack capacitor using the neo-Hookean nonlinear elastic constitutive model for the dielectric material.

(a)

(b)

Fig. 7.   (a) Behavior of the two-stack capacitor in terms of dielectric total displacement under a range of pressures applied. (b) Pressure/capacitance characterization obtained from finite element simulation with the corresponding sensitivity in the case of two-stack capacitor using the neo-Hookean nonlinear elastic constitutive model for the dielectric material.

the same thing for the left electrodes. For a good electrical connection between the armatures, the layers are stacked one on the other and each of them is rotated by a few grades with respect to the lower, in order to avoid short circuits. This layout allows the electrical connection vertically. The use of conductive glues has been chosen to solve a problem regarding the vias fabrication in tactile sensors, in which functional devices from different layers need to be connected by vertical interconnects [27], [34]. Through other common fabrication methods, some works addressed the problem by manually creating vertical feedthrough (creating holes and metalizing them), during or even after the device fabrication [13], [35]. This process is normally conducted in rigid double-layer devices. More difficulties arise in the case of multilayered sensors (more than two layers). The drilling must be done with a perfect cut to ensure that the subsequent metallization contacts all the conductive layers involved. In this way, the vias

making for multilayered sensors is supposed to be easier also because the via itself is not drilled but built like a conductive pillar. Fig. 11(b) shows the vertical section of the three-stack capacitor.

The manufactured three-stacked sensor is shown in Fig. 12.

V. STATIC AND DYNAMIC CHARACTERIZATION

A. Static Characterization: Pressure-Capacitance Measurements

To evaluate the pressure range and the sensitivity of the manufactured capacitive sensors, the electrodes of the sensor were connected to the alligator clips of an LCR meter (GW Instek LCR-6100). We used a mechanical hand-made test rig, shown in Fig. 13, consisting of a vertical steel rod with a plastic cylindrical tip sustained by a linear bearing embedded in the supporting frame. The pressure applied to the capacitor is changed by adjusting the load by applying different weights on the upper supporting structure. For each
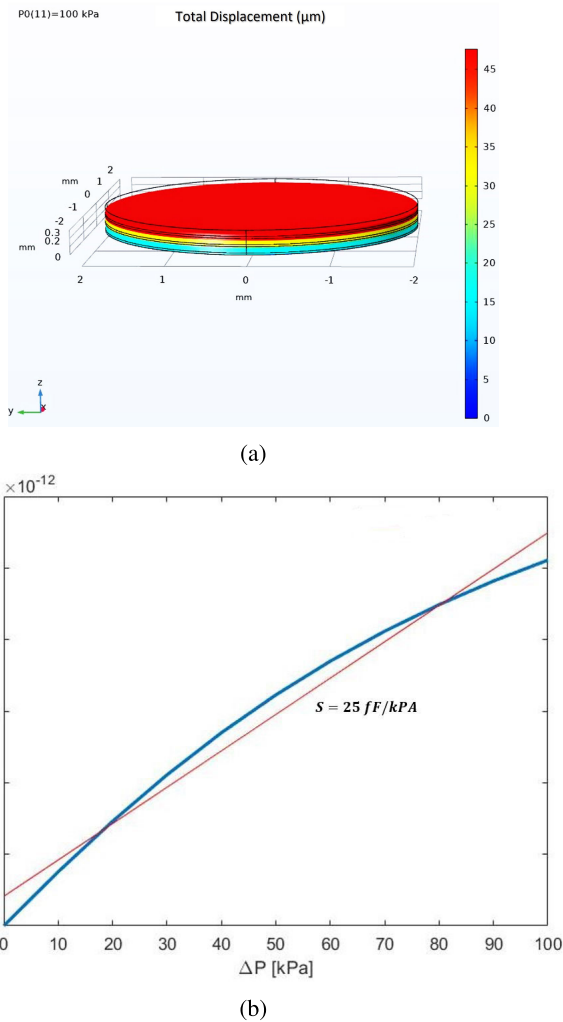
(a)

$S = 25\,fF/kPA$

(b)

Fig. 8. (a) Behavior of the three-stack capacitor in terms of dielectric total displacement under a range of pressures applied. (b) Finite element response with the corresponding sensitivity in the case of the three-stack capacitor using the neo-Hookean nonlinear elastic constitutive model for the dielectric material.
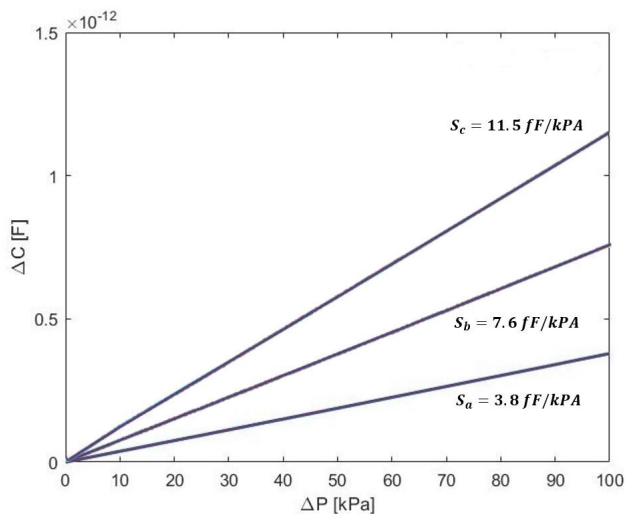

$S_c = 11.5\,fF/kPA$

$S_b = 7.6\,fF/kPA$

$S_a = 3.8\,fF/kPA$

Fig. 9. Finite element response with the corresponding sensitivity in the case of 1) one-stack capacitor, 2) two-stack capacitor, and 3) three-stack capacitor, assuming a linear model for the dielectric material.

experiment, the rod is placed on top of the capacitor and loads are placed until a predetermined pressure (force divided by the
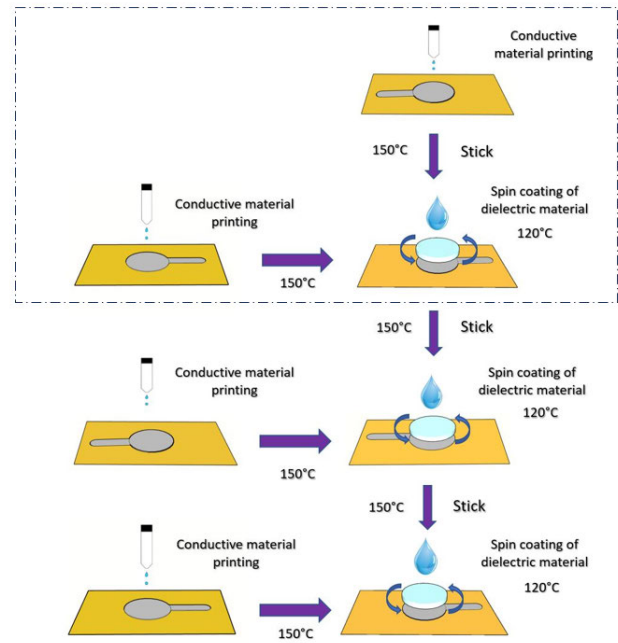
Fig. 10. Schematic illustration of the sensor fabrication process. The dashed rectangle represents the method for a single capacitor. For the three-stacked capacitor, the process must be iterated.

(a)

(b)
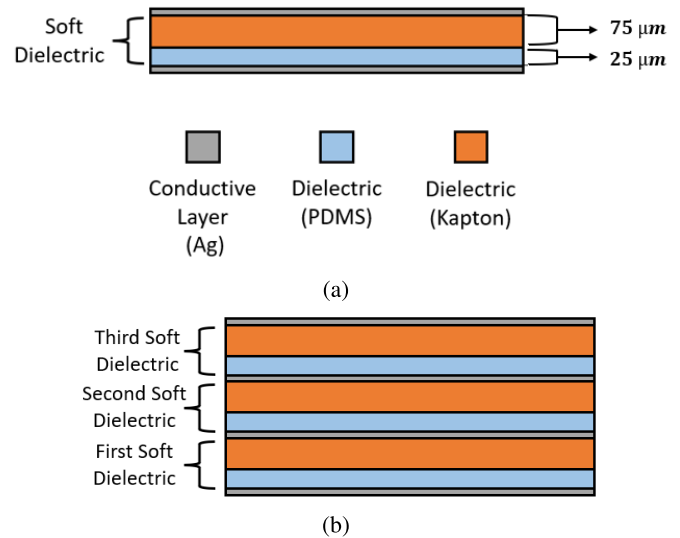
Fig. 11. (a) Vertical section of the structure for single dielectric. (b) Vertical section of the structure for three dielectric layers.

rod surface area) is reached by stacking loads in sequence. Pressures ranging from 10 to 100 kPa were tested, using 14 loads with the same weight. Each load was maintained for 10 s (recording 30 measurements) and then the next load was applied. All the measurements were repeated at least four times. While different loads were being applied, the capacitance of the sensor was measured using the LCR meter with a bias voltage of 1 V at a 1 kHz frequency. In this way, we extracted the capacitance change ΔC of the sensor and its sensitivity S.
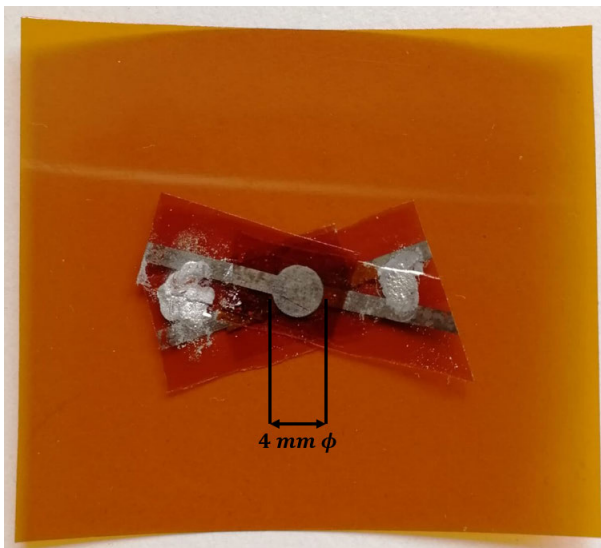
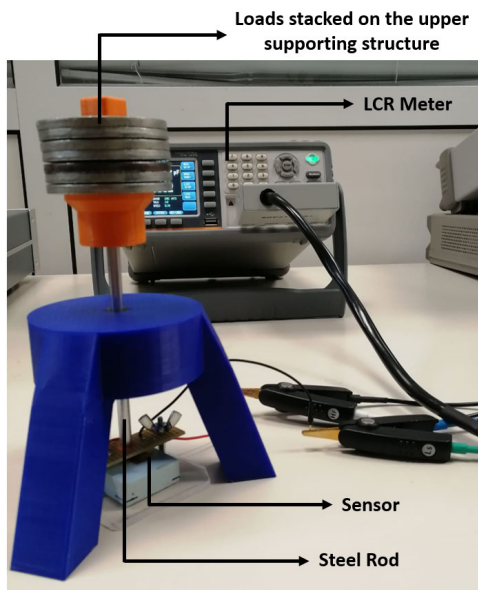Fig. 12. Manufactured 3 stacked capacitive sensor.

Fig. 13. Experimental setup for measuring the change in capacitance in response to applied pressure.

B. Results

We studied the pressure response of the one-stack capacitor, two-stack capacitor, and three-stack capacitor, measuring their corresponding ΔC while the sensors were pressed. Fig. 14(a)–(c) shows the change in capacitance with respect to the applied pressure for each sensor type. Here, the sensitivity has been extracted over two adjacent pressure ranges. The first linear region included pressures from 0 to 30 kPa, whereas the second region included the range from 35 to 100 kPa. As it is possible to notice, in all the cases the sensitivity is higher in the first linear range, and after it decreases as the dielectric layer gets compressed and becomes less compliant. Thus, focusing only on the first linear ranges, the sensitivities for the single capacitor, the two-stack capacitor, and three-stack capacitor are 5.75, 19.3, and 23.7 fF/kPa, respectively. Results show that the
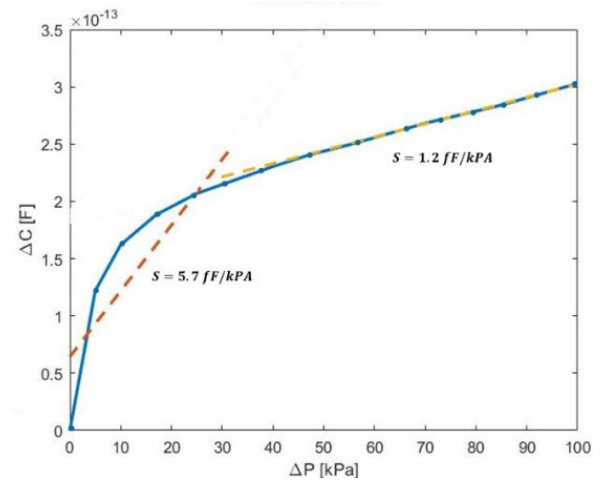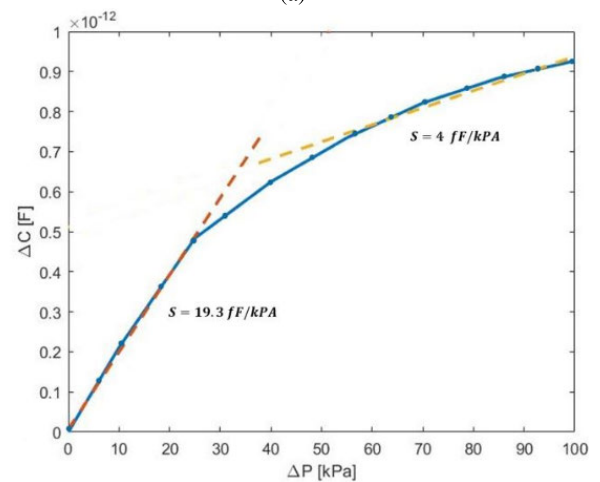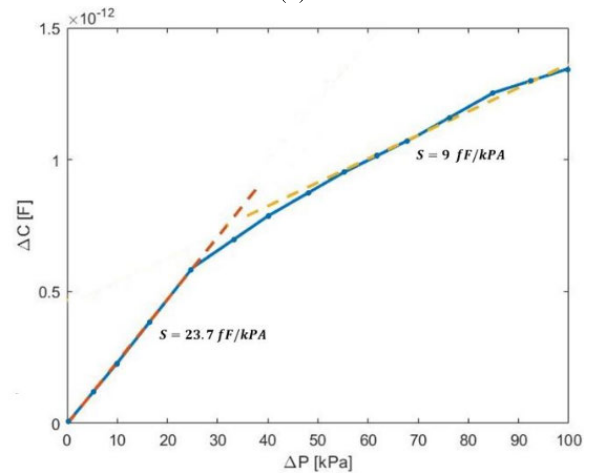
Fig. 14. (a) Experimental sensor output in the case of the one-stack capacitor. Output in terms of ΔC with the corresponding sensitivity in the two regions [0 30 kPa] [35, 100 kPa]. (b) Experimental sensor output in the case of the two-stack capacitor. (c) Experimental sensor output in the case of the three-stack capacitor.

sensitivity has an increase of the 235% passing from a single capacitor to a stack of 2, and an increase of 23% passing from a stack of 2 to a stack of 3 capacitors. The sensitivity
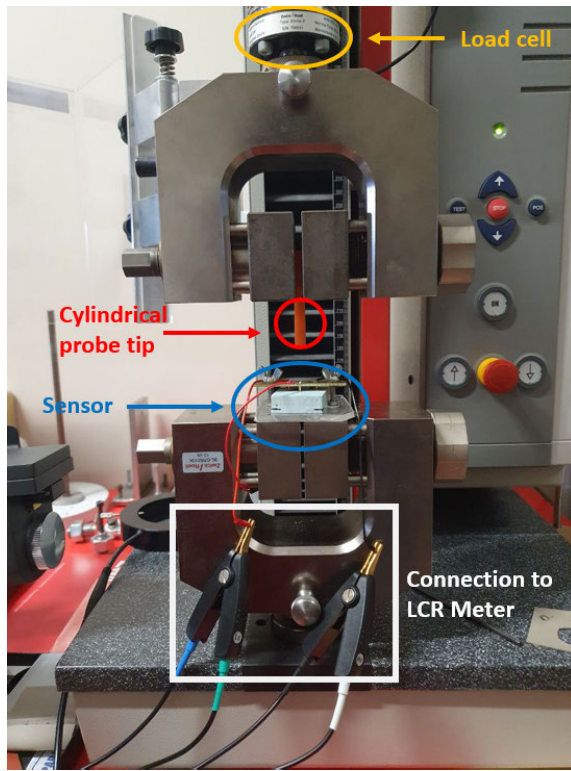
Fig. 15. Experimental setup for measuring the dynamic range of the sensor.

has an increase of 312% if we pass from a single capacitor to a stack made of 3. These outcomes are consistent with the results obtained in simulation as described in Section III-C.

C. Dynamic Characterization: Dynamic Range Response

To measure the dynamic range of the manufactured sensor, we used a materials testing machine (ZwickRoell zwickiLine Z0.5) equipped with a load cell. As shown in Fig. 15, a force is applied on the sensor with a cylindrical probe. At the same time, the sensor is connected to an LCR meter (GW Instek LCR-6100) to measure the variation of capacitance. For each experiment, the cylindrical probe tip is initially set at 2.5 mm above the sensor. During the test, the probe is lowered toward the capacitor at a speed of 0.016 mm/s, until contact is made and the load cell measurements reach a threshold of 1 N. The process has been repeated for five loading-unloading cycles.

D. Results

We analyzed the dynamic range for the one-stack capacitor, two-stack capacitor, and three-stack capacitor. Fig. 16(a)–(c) shows the normalized sensitivity response over time. Here the maximum and minimum values are highlighted to compare the dynamic ranges of the sensors. For the single capacitor, the two-stack capacitor, and three-stack capacitor the sensitivity range is 4, 7%, 10, 4%, and 32, 4%, respectively. These results demonstrate that also the dynamic range of the sensor is definitely higher in the case of parallel capacitors stacked together.
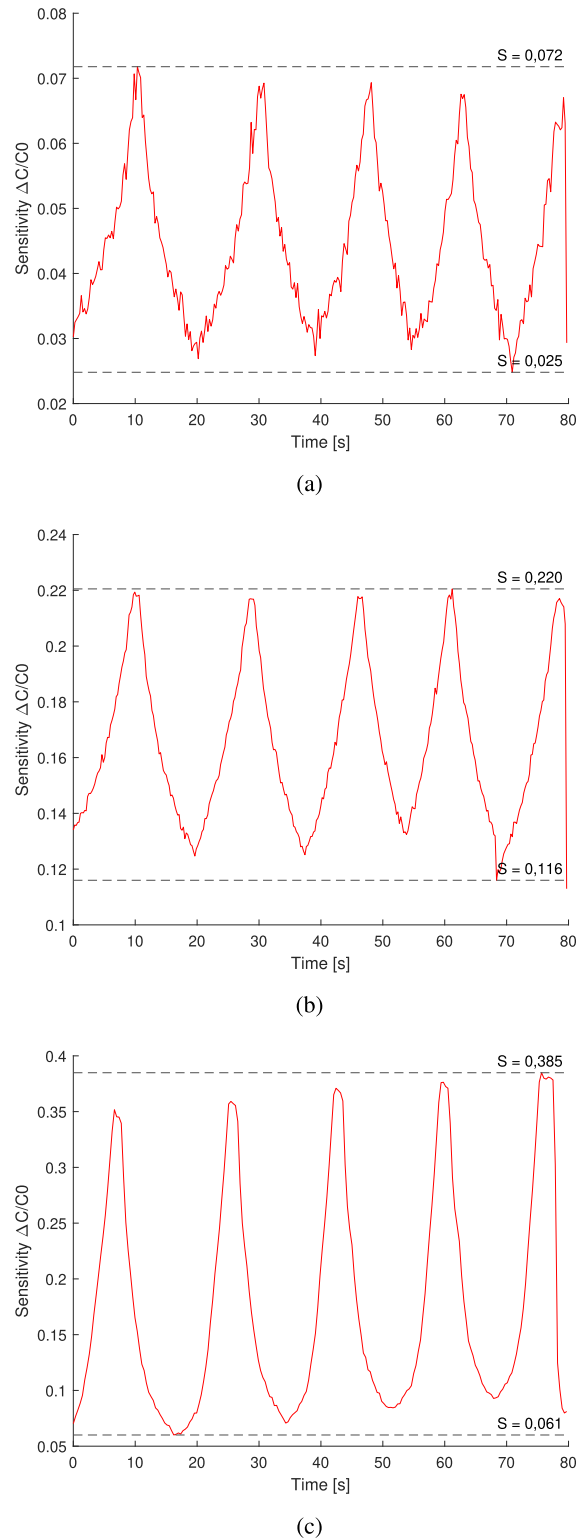

(a)

(b)

(c)

Fig. 16. (a) Experimental sensor output in the case of the one-stack capacitor. Output in terms of sensitivity expressed as $\Delta C/C0$ over the time period of the load-unload cycles. (b) Experimental sensor output in the case of the two-stack capacitor. (c) Experimental sensor output in the case of the three-stack capacitor.

VI. Conclusion

In this work, we have presented a methodology for the design and manufacturing of capacitive tactile sensors. Our experimental results show that vertically stacking multiple capacitances leads to an improvement of the dynamic range
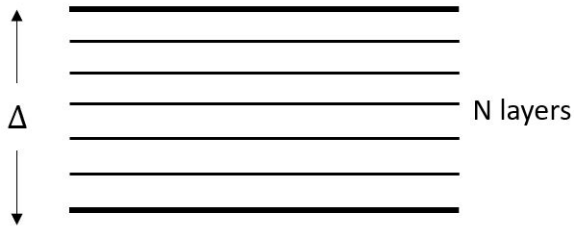
Fig. 17. Generalization for *N* layers.
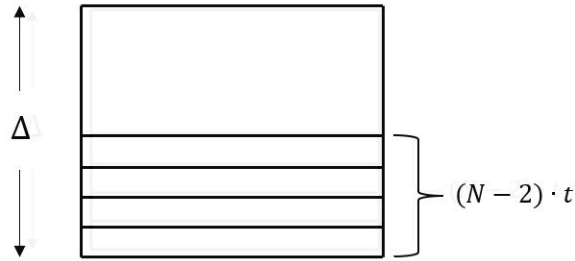
Fig. 18. Case for $N-1$ layers stack.

(from 4, 7% to 32, 4%) and the sensitivity (from 5.75 to 23.7 fF/kPa). Our hypothesis is motivated by the provided simplified model, which allows us to describe mathematically an optimal configuration of the layers composing the stack in order to improve the sensor response. The characteristics of the simplified model have been validated with finite element simulations. The effectiveness of stacked capacitors in a suboptimal configuration has been tested on an inkjet-printed sensor obtained with the proposed fabrication methodology. Indeed the effective physical realization of stacked capacitors is an open research problem. Thus, we propose the experimental realization methodologies in this article as a starting point for further improvements which will be considered as future work.

APPENDIX

As shown in Section II, if we consider the case $N = 2$, where N is a design specification related to the number of layers of the stack, the optimal thickness allocation is $t_{\min}$, $\Delta - t_{\min}$, where Δ is the total transducer thickness intended also as a design specification as shown in Fig. 17 and $t_{\min}$ is a technological constraint representing the minimum possible layer thickness.

$N \cdot t \leq \Delta$ is the feasibility constraint ensuring the possibility of implementing an N-stack capacitor and of course, the interesting case is when $N \cdot t < \Delta$ or even $\Delta \gg N \cdot t$.
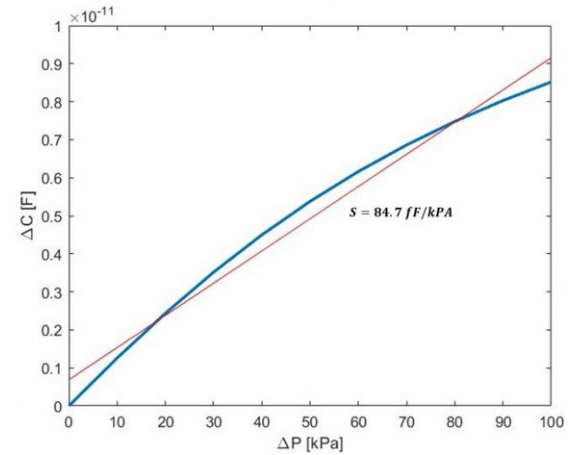
Let assume Δ is given and, by induction, let assume that for a $N - 1$ layers stack (as shown in Fig. 18), the maximum capacitance is obtained using the configuration explained in the following equation:

$$\begin{cases} x_1 = t_{\min} \\ x_{N-2} = t_{\min} \\ x_{N-1} = \Delta - (N-2) \cdot t_{\min}. \end{cases} \quad (20)$$

In the case of N layers we can observe that the distribution of (20) maximizes the capacitance for a vertical space budget
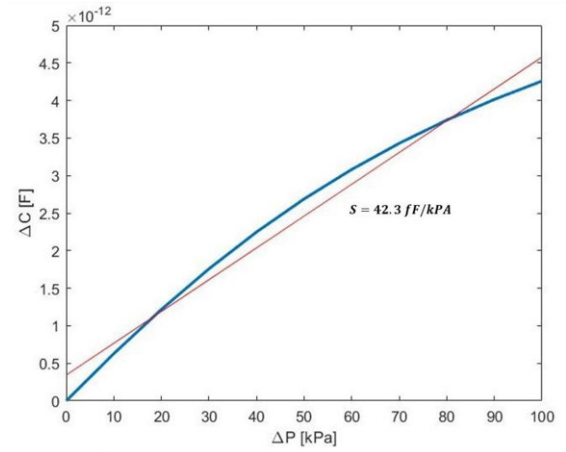
(a)

(b)

Fig. 19.   (a) Prediction on the sensor response in the case of a five-stack capacitor. (b) Prediction on the sensor response in the case of a ten-stack capacitor.

$\Delta_{N-2} = (N - 2) \cdot t_{\min}$. Therefore, for the allocation of the remaining two layers, there is a space budget equal to $\Delta - (N - 2) \cdot t_{\min}$.

This corresponds to the problem of maximizing the capacitance of a two-layers stack for an available space $\bar{\Delta} = \Delta - (N - 2) \cdot t_{\min}$ which leads to the following allocation:

$$\begin{cases} x_{N-1} = t_{\min} \\ x_N = \Delta - (N-2) \cdot t_{\min} + t_{\min}. \end{cases} \quad (21)$$

Here are illustrated the simulations of the sensor's response by increasing the number of capacitors in parallel. The realization of a greater number of layers involves process difficulties and greater encumbrances. In this article, the simulations and the experimental tests have been conducted up to three layers of dielectric. For larger layers, we conducted simulations that give us information on what to expect by increasing the number of parallel capacitors (all the sensors features remain the same in Section III-C). Fig. 19(a) and (b) shows the nonlinear response of a five-stack and ten-stack capacitors. The predictions tell us that by continuing to increase the number of stacks, there are improvements in the variation of the sensor capacitance, which is, therefore, more sensitive.

REFERENCES

[1] X. Wang, L. Dong, H. Zhang, R. Yu, C. Pan, and Z. L. Wang, "Recent progress in electronic skin," *Adv. Sci.*, vol. 2, no. 10, Oct. 2015, Art. no. 1500169, doi: 10.1002/advs.201500169.

[2] P. S. Girão, P. M. P. Ramos, O. Postolache, and J. M. D. Pereira, "Tactile sensors for robotic applications," *Measurement*, vol. 46, no. 3, pp. 1257–1271, Apr. 2013, doi: 10.1016/j.measurement.2012.11.015.

[3] X. Hu et al., "A flexible capacitive tactile sensor array with micro structure for robotic application," *Sci. China Inf. Sci.*, vol. 57, no. 12, pp. 1–6, Dec. 2014, doi: 10.1007/s11432-014-5191-8.

[4] H. Zheng, Y. Jin, H. Wang, and P. Zhao, "DotView: A low-cost compact tactile sensor for pressure, shear, and torsion estimation," *IEEE Robot. Autom. Lett.*, vol. 8, no. 2, pp. 880–887, Feb. 2023, doi: 10.1109/LRA.2022.3233784.

[5] M. Fritzsche, N. Elkmann, and E. Schulenburg, "Tactile sensing: A key technology for safe physical human robot interaction," in *Proc. 6th ACM/IEEE Int. Conf. Human-Robot Interact. (HRI)*, Lausanne, Switzerland, Mar. 2011, pp. 139–140.

[6] R. B. Mishra, N. El-Atab, A. M. Hussain, and M. M. Hussain, "Recent progress on flexible capacitive pressure sensors: From design and materials to applications," *Adv. Mater. Technol.*, vol. 6, no. 4, Apr. 2021, Art. no. 2001023, doi: 10.1002/admt.202001023.

[7] S.-Y. Ke, Y.-W. Chen, and C.-Y. Lo, "Novel response acquisition method for enhancing spatial resolution in capacitive tactile sensing array," *IEEE Sensors J.*, vol. 21, no. 5, pp. 5895–5903, Mar. 2021, doi: 10.1109/JSEN.2020.3043465.

[8] Y.-R. Zhang et al., "Realization of multistage detection sensitivity and dynamic range in capacitive tactile sensors," *IEEE Sensors J.*, vol. 20, no. 17, pp. 9724–9732, Sep. 2020, doi: 10.1109/JSEN.2020.2992484.

[9] Y.-H. Gao, Y.-H. Jen, R. Chen, K. Aw, D. Yamane, and C.-Y. Lo, "Five-fold sensitivity enhancement in a capacitive tactile sensor by reducing material and structural rigidity," *Sens. Actuators A, Phys.*, vol. 293, pp. 167–177, Jul. 2019, doi: 10.1016/j.sna.2019.04.043.

[10] J. Wu et al., "Rational design of flexible capacitive sensors with highly linear response over a broad pressure sensing range," *Nanoscale*, vol. 12, no. 41, pp. 21198–21206, Oct. 2020, doi: 10.1039/d0nr06386j.

[11] Y. Kumaresan, O. Ozioko, and R. Dahiya, "Multifunctional electronic skin with a stack of temperature and pressure sensor arrays," *IEEE Sensors J.*, vol. 21, no. 23, pp. 26243–26251, Dec. 2021, doi: 10.1109/JSEN.2021.3055458.

[12] M. Chandra, S.-Y. Ke, R. Chen, and C.-Y. Lo, "Vertically stacked capacitive tactile sensor with more than quadrupled spatial resolution enhancement from planar arrangement," *Sens. Actuators A, Phys.*, vol. 263, pp. 386–390, Aug. 2017, doi: 10.1016/j.sna.2017.07.004.

[13] Z. Cao, Y. Yuan, G. He, R. L. Peterson, and K. Najafi, "Fabrication of multi-layer vertically stacked fused silica microsystems," in *Proc. 17th Int. Conf. Solid-State Sensors, Actuat. Microsystems*, Jun. 2013, pp. 810–813.

[14] Y.-W. Chen, M. Chandra, and C.-Y. Lo, "Calibrations on shear angle detections in vertically stacked capacitive tactile sensors," *IEEE Sensors J.*, vol. 21, no. 23, pp. 26269–26276, Dec. 2021, doi: 10.1109/JSEN.2021.3069075.

[15] M.-L. Hsieh, S.-K. Yeh, J.-H. Lee, P.-S. Lin, M.-F. Lai, and W. Fang, "Vertically integrated multiple electrode design for sensitivity enhancement of CMOS-MEMS capacitive tactile sensor," in *Proc. 20th Int. Conf. Solid-State Sensors, Actuat. Microsystems Eurosensors*, Jun. 2019, pp. 2174–2177.

[16] Y.-H. Jen et al., "Development and characterization of vertically stacked tactile sensor with hollow structure," *IEEE Sensors J.*, vol. 21, no. 5, pp. 5809–5818, Mar. 2021, doi: 10.1109/JSEN.2020.3037261.

[17] Z. Liu, Z. Yin, Y. Jiang, and Q. Zheng, "Dielectric interface passivation of polyelectrolyte-gated organic field-effect transistors for ultrasensitive low-voltage pressure sensors in wearable applications," *Mater. Today Electron.*, vol. 1, May 2022, Art. no. 100001, doi: 10.1016/j.mtelec.2022.100001.

[18] Z. Yin, M. J. Yin, Z. Liu, Y. Zhang, A. P. Zhang, and Q. Zheng, "Solution-processed bilayer dielectrics for flexible low-voltage organic field-effect transistors in pressure-sensing applications," *Adv. Sci.*, vol. 5, no. 9, Sep. 2018, Art. no. 1701041, doi: 10.1002/advs.201701041.

[19] S. A. Guelcher and J. A. Sterling, "Contribution of bone tissue modulus to breast cancer metastasis to bone," *Cancer Microenvironment*, vol. 4, no. 3, pp. 247–259, Dec. 2011, doi: 10.1007/s12307-011-0078-3.

[20] A. S. LaCroix, S. E. Duenwald-Kuehl, R. S. Lakes, and R. Vanderby, "Relationship between tendon stiffness and failure: A metaanalysis," *J. Appl. Physiol.*, vol. 115, no. 1, pp. 43–51, Jul. 2013, doi: 10.1152/japplphysiol.01449.2012.

[21] P. Maiolino, F. Galantini, F. Mastrogiovanni, G. Gallone, G. Cannata, and F. Carpi, "Soft dielectrics for capacitive sensing in robot skins: Performance of different elastomer types," *Sens. Actuators A, Phys.*, vol. 226, pp. 37–47, May 2015, doi: 10.1016/j.sna.2015.02.010.

[22] T.-H.-L. Le, P. Maiolino, F. Mastrogiovanni, and G. Cannata, "Skinning a robot: Design methodologies for large-scale robot skin," *IEEE Robot. Autom. Mag.*, vol. 23, no. 4, pp. 150–159, Dec. 2016, doi: 10.1109/MRA.2016.2548800.

[23] B. Andó, S. Baglio, V. Marletta, and A. Pistorio, "A contactless inkjet printed passive touch sensor," in *Proc. IEEE Int. Instrum. Meas. Technol. Conf.*, May 2014, pp. 1638–1642.

[24] S. Choi, S. Eom, M. M. Tentzeris, and S. Lim, "Inkjet-printed electromagnet-based touchpad using spiral resonators," *J. Microelectromech. Syst.*, vol. 25, no. 5, pp. 947–953, Oct. 2016, doi: 10.1109/JMEMS.2016.2593956.

[25] T. Yun, S. Eom, and S. Lim, "Paper-based capacitive touchpad using home inkjet printer," *J. Display Technol.*, vol. 12, no. 11, pp. 1411–1416, Nov. 2016, doi: 10.1109/JDT.2016.2598847.

[26] G. Ponraj, S. K. Kirthika, C. M. Lim, and H. Ren, "Soft tactile sensors with inkjet-printing conductivity and hydrogel biocompatibility for retractors in cadaveric surgical trials," *IEEE Sensors J.*, vol. 18, no. 23, pp. 9840–9847, Dec. 2018, doi: 10.1109/JSEN.2018.2871242.

[27] G. Baldini, A. Albini, P. Maiolino, and G. Cannata, "An atlas for the inkjet printing of large-area tactile sensors," *Sensors*, vol. 22, no. 6, Mar. 2022, doi: 10.3390/s22062332.

[28] M. I. Ward and J. Sweeney, "Anisotropic mechanical behaviour," in *An Introduction to the Mechanical Properties of Solid Polymers*, 2nd ed. Hoboken, NJ, USA: Wiley, 2004.

[29] W. Ardi and M. Shingo, "Implementation of Sylgard 184 for powder-based dielectric elastomer actuators," *SEATUC J. Sci. Eng.*, vol. 1, no. 2, pp. 14–19, 2020, doi: 10.34436/sjse.1.2_14.

[30] S. C. B. Mannsfeld et al., "Highly sensitive flexible pressure sensors with microstructured rubber dielectric layers," *Nature Mater.*, vol. 9, no. 10, pp. 859–864, Sep. 2010, doi: 10.1038/nmat2834.

[31] R. Mikkonen, P. Puistola, I. Jönkkäri, and M. Mäntysalo, "Inkjet printable polydimethylsiloxane for all-inkjet-printed multilayered soft electrical applications," *ACS Appl. Mater. Interfaces*, vol. 12, no. 10, pp. 11990–11997, Mar. 2020, doi: 10.1021/acsami.9b19632.

[32] U. G. Lee, W.-B. Kim, D. H. Han, and H. S. Chung, "A modified equation for thickness of the film fabricated by spin coating," *Symmetry*, vol. 11, no. 9, p. 1183, Sep. 2019, doi: 10.3390/sym11091183.

[33] H.-K. Lee, S.-I. Chang, and E. Yoon, "A flexible polymer tactile sensor: Fabrication and modular expandability for large area deployment," *J. Microelectromech. Syst.*, vol. 15, no. 6, pp. 1681–1686, Dec. 2006, doi: 10.1109/JMEMS.2006.886021.

[34] P. Ren and J. Dong, "Direct fabrication of VIA interconnects by electrohydrodynamic printing for multi-layer 3D flexible and stretchable electronics," *Adv. Mater. Technol.*, vol. 6, no. 9, Sep. 2021, Art. no. 2100280, doi: 10.1002/admt.202100280.

[35] Q. Gu, Y. E. Yang, and M. A. Tassoudji, "Modeling and analysis of vias in multilayered integrated circuits," *IEEE Trans. Microw. Theory Techn.*, vol. 41, no. 2, pp. 206–214, Feb. 1993, doi: 10.1109/22.216458.

[36] P. Maiolino, M. Maggiali, G. Cannata, G. Metta, and L. Natale, "A flexible and robust large scale capacitive tactile system for robots," *IEEE Sensors J.*, vol. 13, no. 10, pp. 3910–3917, Oct. 2013, doi: 10.1109/JSEN.2013.2258149.

Giulia Baldini received the B.Sc. and M.Sc. degrees in industrial and biomedical engineering from the Campus Bio-Medico University of Rome, Rome, Italy, in 2017 and 2019, respectively. She is currently pursuing the Ph.D. degree in bioengineering and robotics with the University of Genoa, Genoa, Italy.

Her current research interests are focused on the mechatronic design and development of multimodal tactile sensors for robot bodies, for perception and control, capable to perform handling and manipulation of objects as well as to perform complex interaction operations with humans.

Marco Staiano received the B.Sc. degree in electronic engineering from the University of Modena and Reggio Emilia, Modena, Italy, in 2020, and the M.Sc. degree in robotics engineering from the University of Genoa, Genoa, Italy, in 2022, where he is currently pursuing the National Ph.D. degree in robotics and intelligent machines curriculum Industry 4.0.

His current research is dedicated to the design and development of novel embedded solutions for multimodal tactile sensors on robot bodies to allow safety operations with humans and perform highly sensitive manipulation tasks.

Francesco Grella received the bachelor's degree in biomedical engineering and the master's degree in robotics engineering from the University of Genova, Genoa, Italy, in 2017 and 2019, respectively. He is pursuing the Ph.D. degree in robotics and autonomous systems with the Università degli Studi di Genova, Genoa.

He is a Research Fellow at the Università degli Studi di Genova. His research interests focus on sensor-based robot control, tactile-based robotic perception, and tactile sensor design and fabrication.

Mattia Frascio is a Researcher in mechanical design (RTDa) with the Department of Mechanical, Energy, Management, and Transport Engineering (DIME), University of Genoa, Genoa, Italy. He is also an Associate Researcher at the National Institute for Nuclear Physics (INFN), studying and characterizing the effect of mechanical stress on superconducting materials. Previously, he was a Researcher at the Prosthetics Center-INAIL, Bologna, Italy, focusing on the development of high-functionality prostheses and holding responsibilities for the supervision of funded research projects and for the industrialization of internally developed prototypes. Moreover, he was an Industrial Researcher at CETENA SpA within the European Project TRIM, working on the design of innovative materials applied to the nautical and naval sectors, and an Invited Researcher at the University of Porto, Porto, Portugal, studying the design rules and joining methods for thermoplastic composite polymeric matrix materials, the testing setups for prototypes validation, and their modeling and optimization using finite element analysis (FEA) tools. He possesses expertise in project management and mediation, ensuring the successful implementation of the research project's output. His research is devoted to mechanical design for innovative manufacturing processes and for nonconventional materials, redesign for industrial sustainability, and self-healing and self-sensing for intelligent structures.

Perla Maiolino (Member, IEEE) received the B.Eng. degree in software engineering, the M.Eng. degree in robotics and automation, and the Ph.D. degree in robotics from the University of Genova, Genoa, Italy, in 2006, 2010, and 2014, respectively.

She is an Associate Professor at the Engineering Science Department and a member of Oxford Robotic Institute, University of Oxford, Oxford, U.K., where she is establishing the ORI Soft Robotics Laboratory. She joined the Mechatronic and Automatic Control Laboratory (MACLAB), Department of Informatics, Bioengineering, Robotics and System Engineering (DIBRIS), University of Genova, where as a Ph.D. Student first and then as a Research Fellow, carried out research about new technological solutions for the development and integration of distributed tactile sensors for providing robots with the "sense of touch." Before joining Oxford Robotics Institutes in 2018, she worked as a Postdoctoral Researcher at the Biologically Inspired Robotics Laboratory (BIRL), University of Cambridge, Cambridge, U.K., where she started to be interested in soft robotics pursuing research in soft robot sensing and perception. Her research interests are related to the development of new technological solutions for tactile sensors and robot tactile perception.

Giorgio Cannata (Member, IEEE) received the Laurea degree in electronic engineering from the University of Genoa, Genoa, Italy, in 1988.

He is a Full Professor of Automatic Control at the Polytechnic School of Engineering, University of Genoa. He is the Scientific Coordinator of the Mechatronic and Automatic Control Laboratory (MACLAB), Department of Informatics, Bioengineering, Robotics and System Engineering (DIBRIS), University of Genoa. His current research interests include robotics, mechatronics, and robot sensing and control systems.